JACC: BASIC TO TRANSLATIONAL SCIENCE VOL. 5, NO. 2, 2020


PRECLINICAL RESEARCH

# Genetic Deletion of Socs3 in Smooth Muscle Cells Ameliorates Aortic Dissection in Mice

Saki Hirakata, MD,[a] Hiroki Aoki, MD, PhD,[b] Satoko Ohno-Urabe, MD, PhD,[a] Michihide Nishihara, MD, PhD,[a] Aya Furusho, MD, PhD,[a] Norifumi Nishida, MD,[a] Sohei Ito, MD,[a] Makiko Hayashi, MD,[a] Hideo Yasukawa, MD, PhD,[a] Tsutomu Imaizumi, MD, PhD,[c] Sinichi Hiromatsu, MD, PhD,[d] Hiroyuki Tanaka, MD, PhD,[d] Yoshihiro Fukumoto, MD, PhD[a]

## VISUAL ABSTRACT

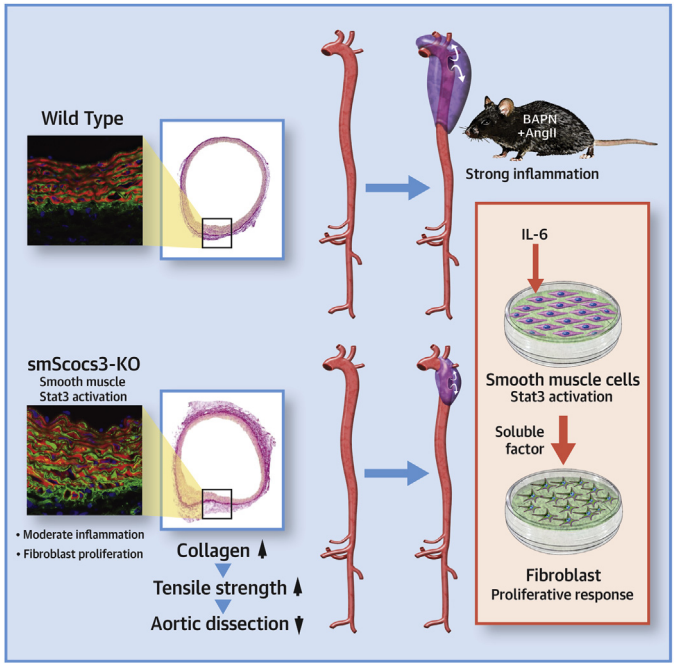


Hirakata, S. et al. J Am Coll Cardiol Basic Trans Science. 2020;5(2):126-44.

## HIGHLIGHTS

- **Stat3, a major signaling molecule for proinflammatory cytokines including IL-6, was activated both in inflammatory cells and in SMC in the aortic walls of human AD and mouse AD model.**
- **SMC-specific deletion of *Socs3* enhanced Stat3 activation in SMC, induced moderate proinflammatory response in the aortic walls, and ameliorated AD in mice.**
- **SmSocs3-KO aortas showed increases in fibroblasts, adventitial collagen fibers, and tensile strength of the aortic walls.**
- **IL-6-stimulated SMC in culture secreted humoral factor(s) that promoted proliferative response of fibroblasts.**

ISSN 2452-302X https://doi.org/10.1016/j.jacbts.2019.10.010

## SUMMARY

Aortic dissection (AD) is the acute destruction of aortic wall and is reportedly induced by inflammatory response. Here we investigated the role of smooth muscle Socs3 (a negative regulator of Janus kinases/signal transducer and activator of transcription signaling) in AD pathogenesis using a mouse model generated via β-aminopropionitrile and angiotensin II infusion. *Socs3* deletion specifically in smooth muscle cells yielded a chronic inflammatory response of the aortic wall, which was associated with increased fibroblasts, reinforced aortic tensile strength, and less-severe tissue destruction. Although an acute inflammatory response is detrimental in AD, smooth muscle-regulated inflammatory response seemed protective against AD. (J Am Coll Cardiol Basic Trans Science 2020;5:126–44) © 2020 The Authors. Published by Elsevier on behalf of the American College of Cardiology Foundation. This is an open access article under the CC BY-NC-ND license (http://creativecommons.org/licenses/by-nc-nd/4.0/).

## ABBREVIATIONS AND ACRONYMS

**AD** = aortic dissection
**AngII** = angiotensin II
**BAPN** = β-aminopropionitrile
**ECM** = extracellular matrix
**IL** = interleukin
**Jnk** = c-Jun N-terminal kinases
**KO** = knockout
**Lox** = lysyl oxidase
**p** = phosphorylated
**SM2** = smooth muscle myosin heavy chain
**SMA** = smooth muscle α-actin
**SMC** = smooth muscle cell
**SMemb** = embryonic isoform of myosin heavy chain
**smSocs3-KO** = knockout of the smooth muscle cell *Socs3*
**Socs** = suppressor of cytokine signaling
**Stat** = signal transducer and activator of transcription
**WT** = wild type

Aortic dissection (AD), which is among the most serious forms of aortic disease, occurs when the intima-media complex in the aortic wall is torn, leading to rapid destruction of the tunica media and the consequent formation of a pseudolumen. The clinical manifestation of AD is abrupt, severe chest or back pain, with no preceding symptoms. In AD involving the ascending aorta—known as a Stanford type A dissection—progression of dissection commonly causes life-threatening complications, including ischemia in critical organs, cardiac tamponade, aortic valve insufficiency, and aortic rupture (1). Type A dissections account for 67% of AD cases according to the IRAD (International Registry of Acute Aortic Dissection) (2), and emergency surgery is recommended in these cases as it can reduce 1-month mortality from 90% to 30% (1). Dissections not involving the ascending aorta are termed Stanford type B dissections. Surgery does not improve mortality rates in type B dissections (1); thus, medical management is recommended over surgery in this situation. Notably, approximately 50% of patients who survive the acute phase of AD experience long-term complications due to progressive destruction of aortic tissue (1). Such long-term complications remain problematic despite substantial advancements in surgical techniques, therapeutic devices, and medical management strategies (3).

SEE PAGE 145

Recent studies have highlighted the importance of destructive inflammation during AD development. Tieu et al. (4) reported a murine model of AD developed by subcutaneously infusing angiotensin II (AngII) into mice. They demonstrated that the proinflammatory cytokine interleukin(IL)-6, together with the monocyte chemoattractant protein1, promoted monocyte infiltration and differentiation into proinflammatory macrophages, ultimately resulting in AD development (4). Other studies have shown that AD development involves proinflammatory responses and tissue destruction, including induction of neutrophil-derived matrix metalloproteinase-9 (5),

From the [a]Division of Cardiovascular Medicine, Department of Internal Medicine, Kurume University School of Medicine, Kurume, Japan; [b]Cardiovascular Research Institute, Kurume University, Kurume, Japan; [c]International University of Health and Welfare, Fukuoka, Japan; and the [d]Division of Cardiovascular Surgery, Department of Surgery, Kurume University School of Medicine, Kurume, Japan. This work was funded, in part, by Grant-in-Aid for Young Scientists 24791398 and 26861116 (awarded to Dr. Hirotaka), Grant-in-Aid for Scientific Research 16K10669 (awarded to Dr. Hirotaka), 21390367, 24390334, 24659640, 26670621, and 16H05428 (awarded to Dr. Aoki) from Japanese Society for the Promotion of Science; grants from the Daiichi Sankyo Foundation of Life Science, the Uehara Memorial Foundation (awarded to Dr. Aoki), the Vehicle Racing Commemorative Foundation (awarded to Dr. Aoki), and Bristol-Myers Squibb (awarded to Dr. Aoki); and Take a New Challenge for Drug Discovery, or TaNeDS, grants from Daiichi Sankyo (awarded to Dr. Aoki). The authors have reported that they have no relationships relevant to the contents of this paper to disclose.

The authors attest they are in compliance with human studies committees and animal welfare regulations of the authors' institutions and Food and Drug Administration guidelines, including patient consent where appropriate. For more information, visit the *JACC: Basic to Translational Science* author instructions page.

Manuscript received September 17, 2019; revised manuscript received October 21, 2019, accepted October 21, 2019.

granulocyte-macrophage colony-stimulating factor (6), and granulocyte colony-stimulating factor (7), as well as the production of reactive oxygen species (8,9). Extracellular matrix (ECM) integrity also seems to be important in AD pathogenesis, as exemplified by the AD susceptibility of mice deficient in ECM components, including collagen-1a and -3a, tenascin C (10–12), and the ECM cross-linking enzyme lysyl oxidase (Lox) (13). Notably, loss of Lox function is causally involved in human AD (14). Compared with healthy tunica media, the tunica media in human AD exhibits lower abundances of collagen (15) and elastin fibers (16). The ECM in the aortic wall is maintained by smooth muscle cells (SMC) and fibroblasts (17), but the roles of these cells and their cell-cell interactions in the context of AD and inflammation remain unclear.

We recently found that mice showed increased susceptibility to AD when they carried a macrophage-specific deletion of *Socs3*, which encodes a negative regulator of the Janus kinases/signal transducer and activator of transcription, or Jak/Stat, pathway (18). This deletion skewed macrophage differentiation toward the proinflammatory M1 phenotype. Additionally, the AD-susceptible phenotype was associated with altered SMC differentiation, suggesting that maladaptive SMC differentiation may be involved in AD pathogenesis. In the present study, we aimed to investigate the molecular mechanism underlying the imbalance in aortic tissue integrity in AD development. Based on the importance of SMC in aortic tissue homeostasis (19), we focused on the role of the suppressor of cytokine signalling-3 (Socs3) in SMC. We generated mice with a specific knockout of the SMC *Socs3* (smSocs3-KO), and then induced AD in smSocs3-KO and wild-type (WT) mice to compare the AD phenotype.

## METHODS

**ANIMAL EXPERIMENTS.** All animal experimental protocols were approved by the Animal Experiments Review Boards of Kurume University. All mice were maintained with normal chow and freely available drinking water, unless otherwise stated. Male mice of 11 to 14 weeks of age were used for all of the animal experiments. We used exclusively male mice because AD predominantly affects men (20). To achieve the smooth muscle–specific deletion of *Socs3,* or smSocs3-KO, we crossed mice that were homozygous for the floxed allele of *Socs3* (*Socs3*$^{fl/fl}$) (21) and that had been backcrossed to C57BL/6J for 3 generations, with *SM22-Cre* mice (JAX Mice, stock no. 004746; The Jackson Laboratory, Bar Harbor, Maine) that carried a Cre recombinase transgene under control of the smooth muscle SM22 promoter. The mice were maintained in the mixed background. *Socs3*$^{fl/fl}$ littermate mice lacking the SM22-Cre transgene served as WT control animals.

A recent report described an AD model induced by administration of β-aminopropionitrile (BAPN) in drinking water for 4 weeks, followed by AngII administration using an osmotic minipump (5). Although this model is excellent for evaluating the mechanism of AD rupture, the high mortality precludes a detailed study of the progression of aortic wall destruction. Additionally, AD induction is achieved by 2 different stimuli with different time courses (long-term BAPN administration and short-term AngII administration), which complicates analysis of the molecular events preceding AD dissection. Here we created a more tunable AD model with simultaneous stimuli for AD induction, to enable evaluation of the molecular events both before and after AD onset. To this end, BAPN (150 mg/kg/day) and AngII (1,000 ng/kg/min) were simultaneously administered using osmotic minipumps (Alzet model 1002, Durect Corporation, Cupertino, California). Mice were anesthetized with 2% isoflurane, and then we implanted 2 pumps: 1 for BAPN and another for AngII. Aortic samples were obtained at the indicated times. Under this experimental condition, the mouse genotype or BAPN+AngII administration did not significantly alter systolic blood pressure, heart rate, or body weight (Supplemental Figure S1). In this model, AD development began approximately 7 days after starting the BAPN+AngII infusion, allowing analyses of tissues and molecular phenotypes before AD development. We empirically determined that this experimental condition could achieve an AD incidence of approximately 70% to 80% within 14 days, thus enabling detection of improvement or worsening of the AD condition.

**MACROSCOPIC ANALYSIS.** Mice were sacrificed by intraperitoneal injection of pentobarbital overdose at the indicated time points, and blood and tissue samples were collected. Perfusion fixation was performed using 4% paraformaldehyde in phosphate-buffered saline at a pressure of 60 cm $H_2O$. To analyze the AD phenotype, we acquired aortic samples before and 14 days after starting the BAPN+AngII infusion. In this model, AD lesions were associated with medial layer disruption (a hallmark of AD) and both intramural and adventitial hematomas, which led to an increased aortic diameter (22). Therefore, we defined an AD lesion as the appearance of an enlarged aortic

section of over 1.5-fold the diameter at the distal end of each segment. The aortic segments included the arch, descending aorta, suprarenal aorta, and infrarenal aorta. The AD lesion length in each segment served as an indicator of the severity of AD-induced tissue destruction.

**CELL CULTURE EXPERIMENTS.** Mouse aortic SMC (no. JCRB0150) were obtained from the National Institutes of Biomedical Innovation, Health and Nutrition (Tokyo, Japan) and maintained in Dulbecco's modified Eagle medium with high glucose and fetal bovine serum. Before starting the experiments, confluent SMC were serum-starved for 24 h, and then incubated for 24 h with or without stimulation with 20 ng/ml recombinant mouse IL-6 (R & D Systems, Minneapolis, Minnesota). After thoroughly washing out IL-6, the SMC were cultured for an additional 24 h to obtain SMC-conditioned media. Confluent NIH3T3 mouse fibroblasts were serum-starved for 24 h, followed by treatment with SMC-conditioned media for 1 h. After thorough washing with phosphate-buffered saline, the cellular proteins were solubilized in radioimmunoprecipitation assay buffer and subjected to immunoblotting.

**PROTEIN EXPRESSION ANALYSIS.** To analyze the morphological and molecular phenotypes before AD development, we obtained aortic samples before and 3 days after starting BAPN+AngII infusion. Aortic tissues were quick-frozen in liquid nitrogen, and then pulverized with an SK mill (Tokken, Kashiwa, Japan). Proteins were extracted using radioimmunoprecipitation assay buffer, and then resolved on a NuPage system (Invitrogen, Thermo Fisher Scientific, Waltham, Massachusetts). Western blots were performed using antibodies specific for Stat3 (no. #4904; Cell Signaling Technology, Danvers, Massachusetts), phospho-Stat3 (pStat3, recognized phospho-Tyr705, no. 9145, Cell Signaling Technology), Jnk (no. ab112501, Abcam, Cambridge, United Kingdom), phospho-Jnk (recognized phospho-Thr183/Tyr185, no. 4671, Cell Signaling Technology), Smad2 (no. 5339, Cell Signaling Technology), phospho-Smad2 (no. 3108, Cell Signaling Technology), Lox (no. ab31238, Abcam), cyclin D3 (no. 2936, Cell Signaling Technology), and phosphotyrosine (PY20, no. ab16389, Abcam).

**TISSUE STAINING AND IMAGING CYTOMETRY.** Paraformaldehyde-fixed, paraffin-embedded tissue sections were immunostained with antibodies specific for α-smooth muscle actin (SMA) (no. A5228, Sigma-Aldrich, St. Louis, Missouri), pStat3 (no. 9145, Cell Signaling Technology), and Ki67 (no. ab16667, Abcam). To assess collagen deposition, the tissue sections were processed to enable picrosirius red staining. We used fresh-frozen and optical coherence tomography–embedded sections to perform immunostains with antibodies specific for the fibroblast marker ER-TR7 (no. sc-73355, Santa Cruz Biotechnology, Dallas, Texas) and SMA (no. A5228, Sigma-Aldrich).

Tissue samples that were double stained for either SMA and phospho-Smad2 (no. 3108, Cell Signaling Technology) or SMA and Ki67 were analyzed by imaging cytometry on an ArrayScan XTI (Thermo Fisher Scientific), followed by data analysis using FlowJo software (FlowJo LLC, Ashland, Oregon). The staining conditions were determined by staining with a single antibody and were validated when we observed identical results with 3-color staining. All samples in a given set of analyses were processed simultaneously, under the same staining conditions, and photomicrographs were acquired under the same exposure conditions to obtain consistent results. In the imaging cytometry analyses using the ArrayScan XTI, each cell was identified by nuclear 4',6-diamidino-2-phenylindole staining, and was then arbitrarily gated to separate the positive (SMC) and negative (non-SMC) populations, based on SMA signals surrounding the nucleus. We also arbitrarily determined the gates for detecting the nuclear signal intensity of pStat3 or Ki67. These gates remained constant for all experimental groups in a given set of analyses. Each experimental group included 3 mice, and we obtained 2 aortic sections from each mouse. All of the counted cells were combined to generate a histogram.

**TRANSCRIPTOME ANALYSIS.** From aortic samples that had been quick-frozen in liquid nitrogen, we extracted total ribonucleic acid using TRIzol (Invitrogen) and the RNeasy kit (Qiagen, Hilden, Germany), following the manufacturers' instructions. Transcriptome analyses were performed with a SurePrint G3 Mouse GE microarray 8x60K (Agilent Technologies, Santa Clara, California). We obtained functional annotation clusters from the DAVID (Database for Annotation, Visualization, and Integrated Discovery, version 6.8) (23,24), with the Gene Ontology terms set to GOTERM_BP_FAT, GOTERM_CC_FAT, and GOTERM_MF_FAT.

**HUMAN AD TISSUE.** All human specimens were obtained with informed consent from the patients, and all protocols involving human specimens were

**FIGURE 1** **Activation of Stat3 in AD**

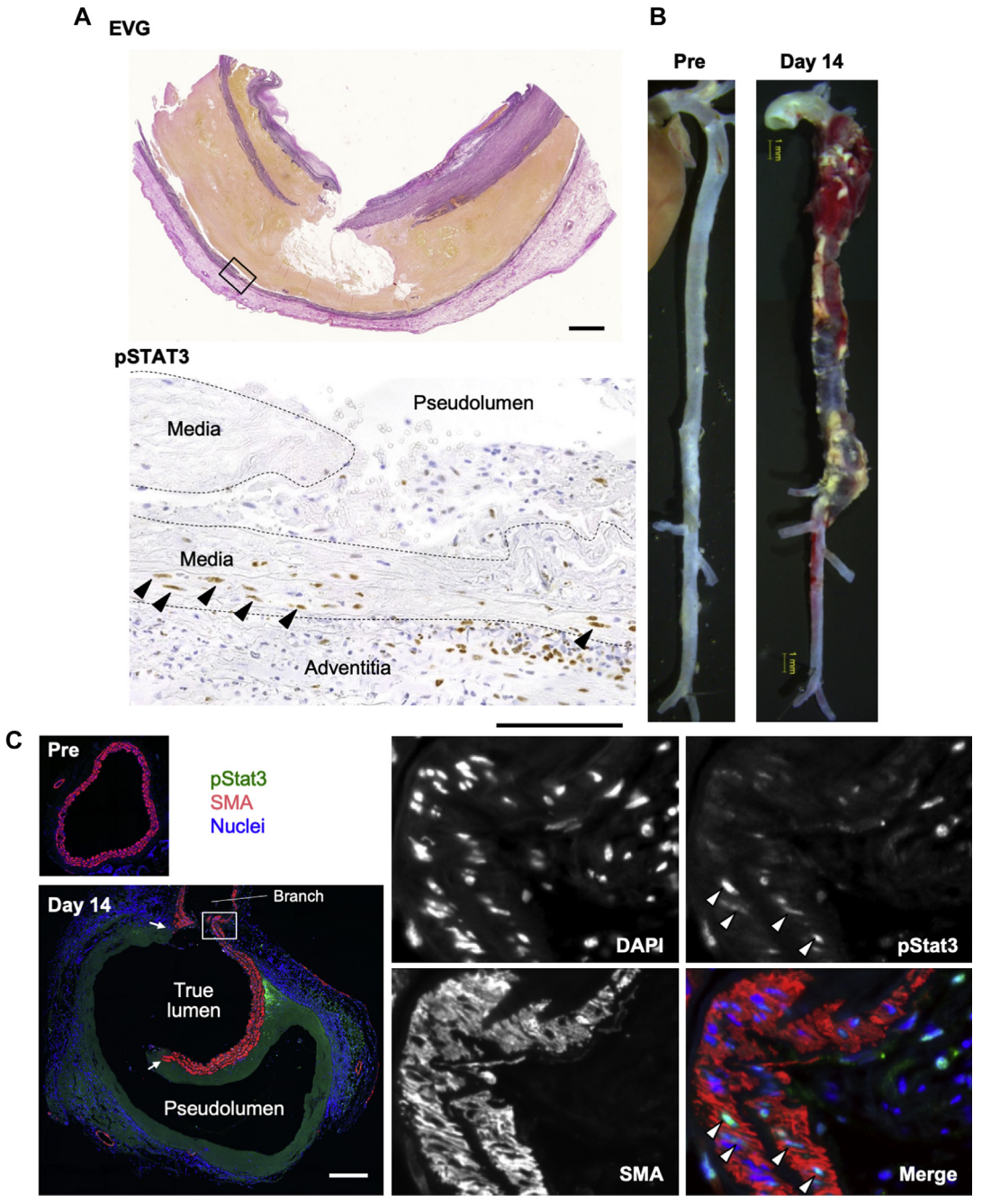


**(A)** Representative images of a human aortic dissection (AD). **(Top)** Elastica Van Gieson (EVG) staining reveals a break in the aortic wall. **Rectangle** indicates the area magnified in the **bottom panel**. **(Bottom) Brown** color indicates immunohistochemical staining of activated phosphorylated signal transducer and activator of transcription-3 (pSTAT3). Bars = 2 mm for EVG and 0.5 mm for pSTAT3. **(B)** Macroscopic images of normal aorta (Pre) and aorta from the AD model after 14 days of β-aminopropionitrile plus angiotensin II infusion (day 14). Bar **(yellow)** = 1 mm. **(C)** Representative images of aortic section from normal aorta (Pre) and a mouse AD model on day 14, immunostained to show pStat3 **(green)** and α-smooth muscle actin (SMA) **(red)** expression. Nuclei were stained with 4′,6-diamidino-2-phenylindole (DAPI) **(blue)**. **Arrows** indicate media breakage. **White rectangle** in the left panel indicates the area of the magnified images in the **right panels**. **Arrowheads** indicate pStat3-positive nuclei in smooth muscle cells. Bar = 200 μm.

approved by the Institutional Review Board at Kurume University Hospital. Human AD tissue was obtained from patients during surgery for AD. Aortic tissues were fixed in 4% paraformaldehyde, paraffin-embedded, and sliced into 5-μm-thick tissue sections. The tissue sections were processed for either elastica Van Gieson staining or immunohistochemical staining with antibodies specific for pStat3 (no. 9145, Cell Signaling Technology).

**MECHANICAL PROPERTIES OF THE AORTIC WALLS.** To assess the mechanical properties of the aortic wall, we devised a blood vessel tensile tester. Briefly, an aortic ring was immersed in phosphate-buffered saline containing 10 mmol/l 2,3-butanedione monoxime to suppress SMC contraction (25), and placed around 2 tungsten rods (0.25-mm diameter) set at opposite sides of the ring. The rods were pulled apart at a constant speed (0.1 mm/s) under a microscope equipped with a video camera, a force gauge, and an actuator, connected to a controller. We simultaneously recorded signals from the force gauge and video camera (Supplemental Figure S2A). Aortic rings were obtained from the end of the aortic arch, distal to the branch point at the left subclavian artery, and were cut to a width of 2 mm. Based on the simultaneous video and force recordings, we found that the sharp and blunt peaks in the force record indicated the maximal tensile forces of the medial layer and the adventitial layer, respectively (Supplemental Figures S2B and C).

**STATISTICAL ANALYSES.** Animals were randomly assigned to the experimental groups, and animal experimental data were acquired by researchers or technicians who were blinded to the genetic modification and experimental interventions. Statistical analyses were performed using GraphPad Prism (version 5, GraphPad Software, San Diego, California). We tested normality with the D'Agostino and Pearson normality test, and then evaluated the data using Bartlett test for equal variances. Normally distributed data were analyzed using 1-way analysis of variance to compare 3 or more groups, and those not normally distributed were evaluated using the Kruskal-Wallis test, followed by Bonferroni multiple comparison test. Data are shown as mean ± SEM. A p value of $<0.05$ was considered statistically significant.

## RESULTS

**STAT3 ACTIVATION IN AD.** We first examined STAT3 activation in human AD tissue (**Figure 1A**) and detected activated phosphorylated (p) STAT3 (pSTAT3) in the adventitial and medial layers of the damaged aortic wall. Phosphorylated STAT3-positive medial cells with elongated nuclei exhibited orderly layering between the elastic lamellae, indicating that they were SMC. We next examined Stat3 activation in our mouse AD model induced via continuous infusion of BAPN+AngII (**Figure 1B**). Immunofluorescence staining revealed Stat3 activation in both SMC of the media and non-SMC in the adventitia (**Figure 1C**).

We created a mouse AD model by treating both WT and smSocs3-KO mice with continuous infusion of BAPN+AngII (**Figure 1**, Supplemental Figure S3). To investigate phenomena before AD development, we analyzed morphologically intact aorta samples before and 3 days after starting BAPN+AngII infusion. The aortic sections were labeled with antibodies against pStat3 and SMA (**Figure 2**), and imaging cytometry analysis revealed a higher proportion of SMA-negative non-SMC in the smSocs3-KO aortas compared with in the WT aortas, both at baseline (pre-infusion) and after 3 days of BAPN+AngII infusion. Among the total cell population, the baseline proportion of pStat3-positive cells was higher in smSocs3-KO samples (10.0%) than in WT samples (6.7%). BAPN+AngII infusion induced a slight increase in the pStat3-positive population in WT samples (from 6.7% to 8.5%) and a greater increase in smSocs3-KO samples (from 10.0% to 18.8%). In the smSocs3-KO aortic samples, the pStat3-positive population increased among both SMA-positive SMC (from 1.4% to 8.9%) and SMA-negative non-SMC (from 27.0% to 33.0%). These results indicated that *Socs3* deletion in SMC caused Stat3 activation in both SMC and non-SMC. Moreover, this effect was enhanced by BAPN+AngII treatment. *Socs3* deletion in SMC also led to increased non-SMC in the aorta.

**ROLE OF SMOOTH MUSCLE SOCS3 IN AD PATHOGENESIS.** Next, we evaluated the macroscopic phenotype of AD in WT and smSocs3-KO mice. BAPN+AngII infusion induced AD development in 10 of 12 WT mice and 6 of 8 smSocs3-KO mice, with no significant difference between the 2 groups. We divided the aorta into 4 parts: the aortic arch and ascending aorta; descending thoracic aorta; suprarenal aorta; and infrarenal aorta (**Figure 3**). To evaluate the severity of AD-induced aortic wall destruction, we measured the lengths of aortic lesions that caused vessel enlargement to over 1.5-fold the reference

**FIGURE 2** **Effects of SMC-Specific *Socs3* Deletion on Stat3 Activation**

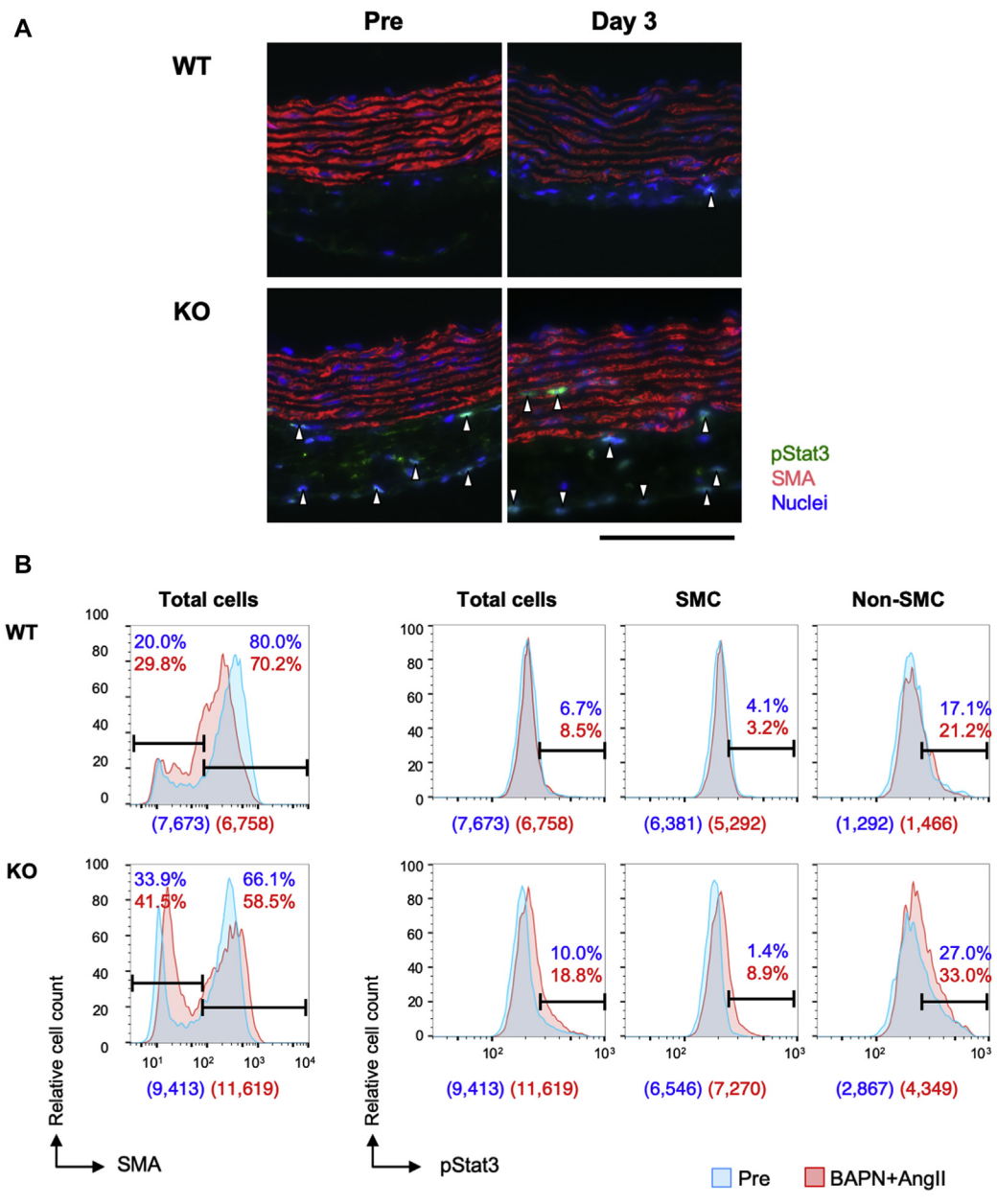


**(A)** Representative images of mouse aortas with immunofluorescent staining to show expressions of pStat3 **(green)**, SMA **(red)**, and nuclei (DAPI; **blue**). Aortic samples were obtained from wild-type (WT) or smooth muscle Socs3-knockout (KO) mice, before (Pre) and after (day 3) continuous β-amino-propionitrile plus angiotensin II (BAPN+AngII) infusion. **Arrowheads** indicate pStat3-positive nuclei. All samples are shown with the luminal side up, adventitial side down. Bar = 100 μm. **(B)** Imaging cytometry results for aortic tissues stained with **(left)** SMA and **(right)** pStat3 (as in **A**). Upper and lower histograms show results for WT and KO aortas, respectively, before (Pre) **(blue)** and after 3 days of BAPN+AngII infusion **(red)**. **(Left)** SMA detection: negative staining indicates non–smooth muscle cells (SMC) and positive staining indicates SMC, as defined with arbitrarily delineated gates **(horizontal bars)** that remained constant for all samples. **(Right)** pStat3 detection among all aortic cells (total cells), SMC, and non-SMC. Percentage values indicate the proportions of cells within the gated sections among all the analyzed cells in Pre **(blue)** and BAPN+AngII **(red)** samples. Numbers in parentheses under each histogram indicate the counted cell numbers without **(blue)** and with **(red)** BAPN+AngII. Abbreviations as in Figure 1.

diameter in each portion of the aorta. In this model, the infrarenal aorta did not show AD development. The aortic arch exhibited significantly more severe tissue destruction in WT mice (2.463 ± 0.456; n = 12) compared with that in smSocs3-KO mice (0.426 ± 0.302 mm; n = 8; p = 0.011). These results indicated that *Socs3* deletion in SMC prevented AD aggravation in the aortic arch, but did not affect AD prevalence.

To investigate the molecular mechanism underlying the smSocs3-KO phenotype, we performed transcriptome analyses and functional annotation analyses in DAVID (25). We focused on the genes that showed changes in expression that differed between WT and smSocs3-KO at baseline (before BAPN+AngII). Among the 55,681 probes in the deoxyribonucleic acid microarray, 337 genes showed increased expression (fold change >2; $p < 0.05$) (Supplemental Table S1) and 132 genes showed decreased expression (fold change <0.5; $p < 0.05$) (Supplemental Table S2) in smSocs3-KO mice compared with in WT mice. Functional annotation analyses revealed that the genes with higher expression in smSocs3-KO aortas were located in 4 annotation clusters, comprising 167 genes with enrichment scores over 3 (**Table 1**). Representative Gene Ontology terms for these clusters were "response to cytokines," "extracellular space," "defense response," "immune response," and "inflammatory response." Among genes that were suppressed in smSocs3-KO aortas, the highest enrichment score was only 1.49. Therefore, we did not attribute specific functions to this set of genes. These findings suggested that *Socs3* deletion in SMC caused activation of the inflammatory response and changes in the extracellular environment in the aorta. Notably, the pattern of gene expression changes observed in smSocs3-KO aorta showed significant correlation with the pattern induced by BAPN+AngII challenge ($p < 0.001$; $R^2 = 0.229$; slope, 0.322 ± 0.020) (Supplemental Figure S4), indicating that *Socs3* deletion in SMC yielded a response similar to the changes induced by BAPN+AngII, albeit to a lesser extent.

To verify the transcriptome findings, we performed quantitative reverse transcription polymerase chain reaction analysis of selected genes (**Figure 4**) with altered expressions among the experimental groups. We also evaluated the inflammatory response by examining the expressions of macrophage and T-cell subset markers. Aorta samples from smSocs3-KO mice exhibited induction of messenger ribonucleic acids encoding the acute phase proteins IL-6, serum amyloid A3, and lipocalin-2, supporting the notion that *Socs3* deletion in SMC caused inflammatory response activation. With regard to macrophage markers, BAPN+AngII induced *Cd68* in both WT and smSocs3-KO and induced the M1 macrophage marker *Cd80* only in WT. The M2 macrophage marker *Cd206* was induced at baseline in smSocs3-KO. In the presence of BAPN+AngII, expression of the M2 marker *Cd163* was higher in smSocs3-KO than in WT, suggesting M2-skewed macrophage differentiation in the smSocs3-KO aorta. Among T-cell markers, the

**TABLE 1 Functional Annotation Clusters for Genes That Were Up-Regulated in smSocs3-KO Aortas**

| GO Terms | Gene Count | p Value |
|---|---|---|
| Annotation cluster 1 (enrichment score: 4.64) | | |
| GO:0034097, response to cytokine | 32 | <0.001 |
| GO:0071345, cellular response to cytokine stimulus | 21 | <0.001 |
| GO:0071310, cellular response to organic substance | 46 | 0.005 |
| Annotation cluster 2 (enrichment score: 3.91) | | |
| GO:0005615, extracellular space | 57 | <0.001 |
| GO:0005576, extracellular region | 105 | <0.001 |
| GO:0044421, extracellular region part | 89 | <0.001 |
| GO:0070062, extracellular exosome | 60 | 0.003 |
| GO:1903561, extracellular vesicle | 60 | 0.003 |
| GO:0043230, extracellular organelle | 60 | 0.004 |
| GO:0031988, membrane-bounded vesicle | 71 | 0.009 |
| Annotation cluster 3 (enrichment score: 3.65) | | |
| GO:0006952, defense response | 49 | <0.001 |
| GO:0006955, immune response | 39 | <0.001 |
| GO:0002682, regulation of immune system process | 36 | <0.001 |
| GO:0002684, positive regulation of immune system process | 26 | <0.001 |
| GO:0045087, innate immune response | 22 | <0.001 |
| GO:0050776, regulation of immune response | 21 | <0.001 |
| Annotation cluster 4 (enrichment score: 3.63) | | |
| GO:0006952, defense response | 49 | <0.001 |
| GO:0006954, inflammatory response | 28 | <0.001 |
| GO:0050727, regulation of inflammatory response | 14 | <0.001 |
| GO:0032101, regulation of response to external stimulus | 24 | <0.001 |
| GO:0050729, positive regulation of inflammatory response | 8 | 0.001 |
| GO:0031349, positive regulation of defense response | 12 | 0.003 |
| GO:0031347, regulation of defense response | 19 | 0.004 |
| GO:0080134, regulation of response to stress | 27 | 0.027 |

GO = Gene Ontology; smSocs3-KO = knockout of the smooth muscle cell *Socs3*.

**FIGURE 3 Effects of SMC-Specific *Socs3* Deletion on AD**

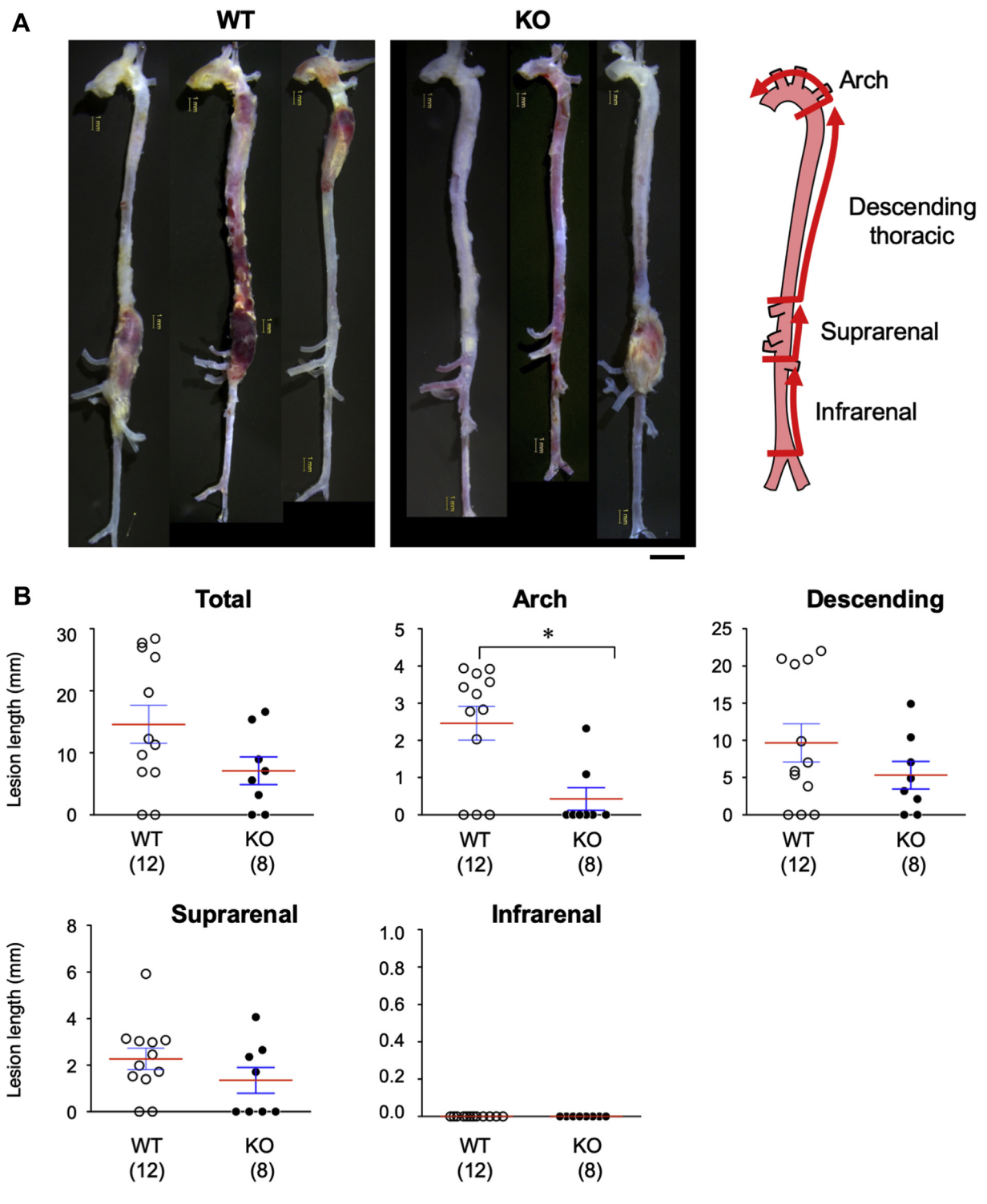


Representative images show aortas from AD models induced in **(left)** WT and **(middle)** KO mice. **(Right)** We assessed the lengths of AD lesions in the depicted aortic segments: the arch and ascending aorta, descending thoracic, suprarenal, and infrarenal aorta. Bars = 1 mm **(yellow)** and 2 mm **(black)**. **(B)** Quantitative analysis of the lengths (mm) of tissue destruction lesions found in the indicated aortic segments. The numbers of mice in each group are shown in parentheses. **Red bars** indicate mean values. *$p < 0.05$. Abbreviations as in Figures 1 and 2.

**FIGURE 4 Expression Analysis of the Selected Genes**

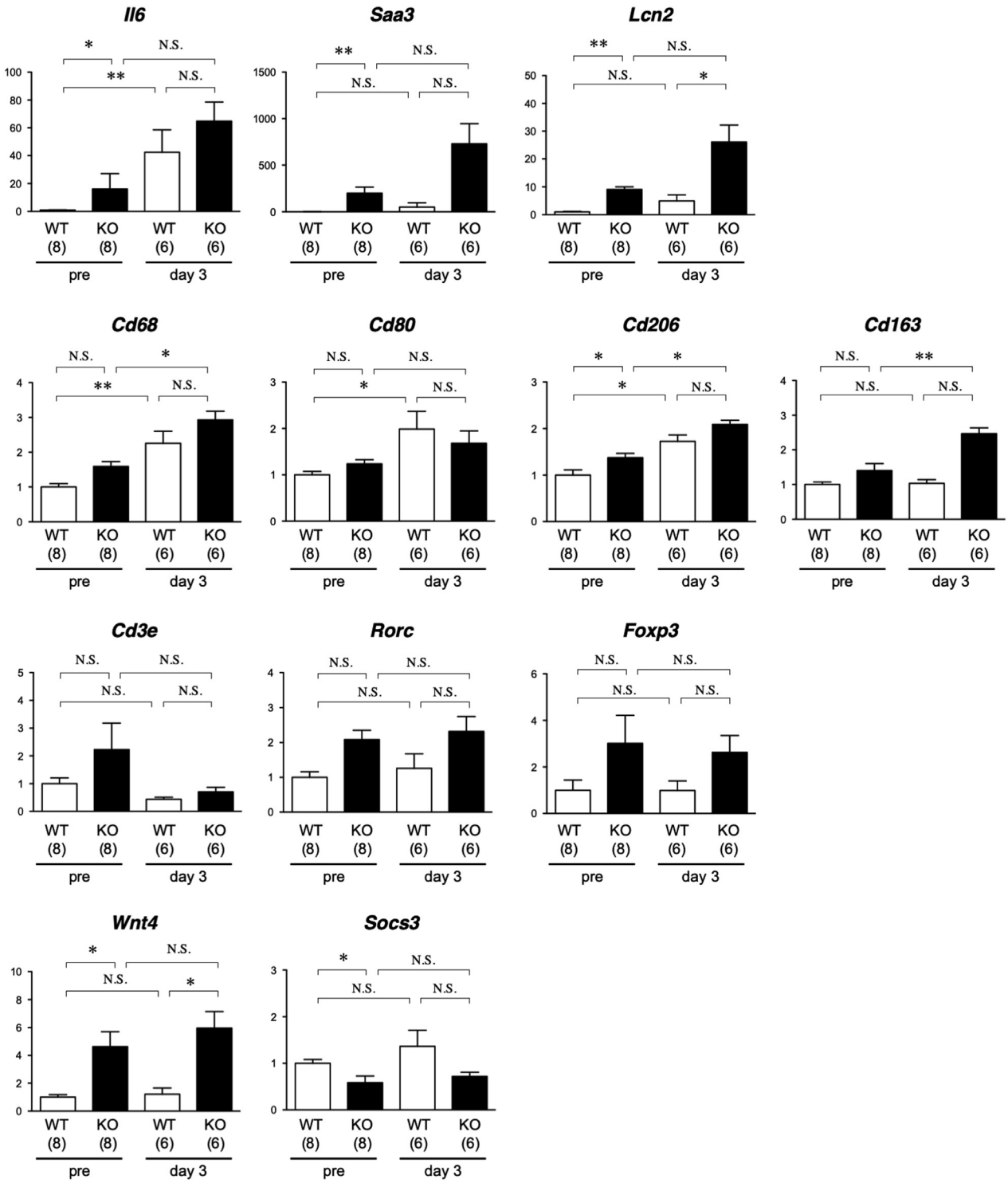


Analysis of messenger ribonucleic acid expression before and 3 days after BAPN+AngII treatment in aortic tissue from WT **(open columns)** and KO **(solid columns)** mice. The data were normalized against *Gapdh* expression as an internal control and expressed relative to the WT samples without any intervention (pre). The numbers of mice in each group are shown in parentheses. *$p < 0.05$; **$p < 0.01$. NS = not significant; other abbreviations as in Figure 2.

pan-T-cell marker *Cd3e*, T helper 17 cell marker *Rorc*, and regulatory T marker *Foxp3* showed a trend of increased expression in the smSocs3-KO aorta, although none of these differences reached statistical significance. The smSocs3-KO aorta also showed higher expression of *Wnt4*, which reportedly promotes myofibroblast differentiation and fibrosis (26). *Socs3* expression was lower in smSocs3-KO samples, possibly reflecting the effective *Socs3* deletion in SMC of the aortic tissue.

**SIGNALING PATHWAYS AND SMC PHENOTYPE IN THE AORTA.** We performed Western blots with samples from WT and smSocs3-KO aortas isolated before and 3 days after BAPN+AngII infusion (**Figure 5**). Using specific antibodies, we examined signaling pathways involved in inflammation, ECM metabolism, and the cell cycle—which contribute to the molecular pathogenesis of AD (18,27). Stat3 activity was significantly higher in smSocs3-KO aortas than in WT aortas, indicating that smooth muscle *Socs3* deletion effectively activated the Stat3 pathway in the aorta in vivo. This Stat3 activation was accompanied by c-Jun N-terminal kinases (Jnk) activation. Jnk expression and activity levels in the aorta tended to be higher after BAPN+AngII challenge than pre-challenge, but these differences were not statistically significant.

At 3 days after BAPN+AngII infusion, WT aortas exhibited significantly increased expression levels of Smad2, Lox, and cyclin D3. Consistently, in WT aortas, BAPN+AngII infusion led to increased expression of embryonic isoform of myosin heavy chain (SMemb), a marker for the synthetic phenotype of SMC. Matrix metalloproteinase-2 and -9 were undetectable with gelatin zymography, even after prolonged incubation of the gel for 3 days. These findings revealed that 3 days of BAPN+AngII challenge induced activation of the cell cycle, ECM synthesis, and phenotypic modulation of SMC toward the embryonic phenotype. However, infusion did not induce significant inflammatory or tissue-destructive responses in the WT aortas at this time point.

In contrast to WT aortas, smSocs3-KO aortas did not exhibit changes in cyclin D3 or Lox expression following BAPN+AngII infusion. Notably, compared with WT aortas, smSocs3-KO aortas showed higher expression levels of both smooth muscle myosin heavy chain (SM2, a marker for the contractile phenotype of SMC) and SMemb. However, BAPN+AngII infusion did not alter the SM2 or SMemb expression levels in smSocs3-KO aortas. These findings suggested that, although the baseline inflammatory response was higher in smSocs3-KO aortas than in WT aortas, the smSocs3-KO aortas were insensitive to the BAPN+AngII challenge.

**CELLULAR COMPOSITION AND PROLIFERATIVE RESPONSE IN AD.** To observe the early response during AD development, we double stained samples to detect SMA and the proliferative cell marker Ki67 in WT and smSocs3-KO aortas, with or without BAPN+AngII infusion (**Figure 6**). The histogram of SMA signals showed that approximately 80% of WT aortic wall cells were SMA-positive SMC. BAPN+AngII infusion caused a slight increase of non-SMC, concomitant with reduced SMA expression within the SMA-positive population. In smSocs3-KO aortas, over 30% of aortic wall cells were SMA-negative non-SMC at baseline. Ki67 signals indicated that the cell proliferative response was negligible at baseline in WT aortas. BAPN+AngII treatment led to increased Ki67-positive cells in the SMA-negative population, from 4.9% at baseline to 26.7% after infusion. At baseline, the Ki67-positive cell population was slightly larger in smSocs3-KO aortas (2.4%) compared with in WT aortas (1.2%). After BAPN+AngII treatment, the cell proliferative response was lower in smSocs3-KO aortas than in WT aortas, among both SMC (1.0% smSocs3-KO vs. 2.4% WT) and non-SMC (16.6% smSocs3-KO vs. 26.7% WT). These findings indicated that non-SMC were more abundant in smSocs3-KO aortas than in WT aortas before BAPN+AngII infusion, and that smSocs3-KO aortas exhibited a blunted cell proliferative response following BAPN+AngII infusion.

**ELEVATED COLLAGEN DEPOSITION AND AORTIC TENSILE STRENGTH IN smSocs3-KO MICE.** The above-described results indicated that the baseline proportion of non-SMC was higher in smSocs3-KO aortas compared with in WT aortas. To identify the cell types within this SMA-negative population, we stained aortas with antibodies specific for various cell-type markers. The fibroblast marker ER-TR7 stained more intensely in the adventitia and part of the media in smSocs3-KO compared with in those regions in WT samples (**Figure 7A**). We next used picrosirius red staining to detect collagen fibers in WT and smSocs3-KO aortas, before and after BAPN+AngII treatment (**Figure 7B**). Collagen

**FIGURE 5 Protein Expression Levels Before AD Development**

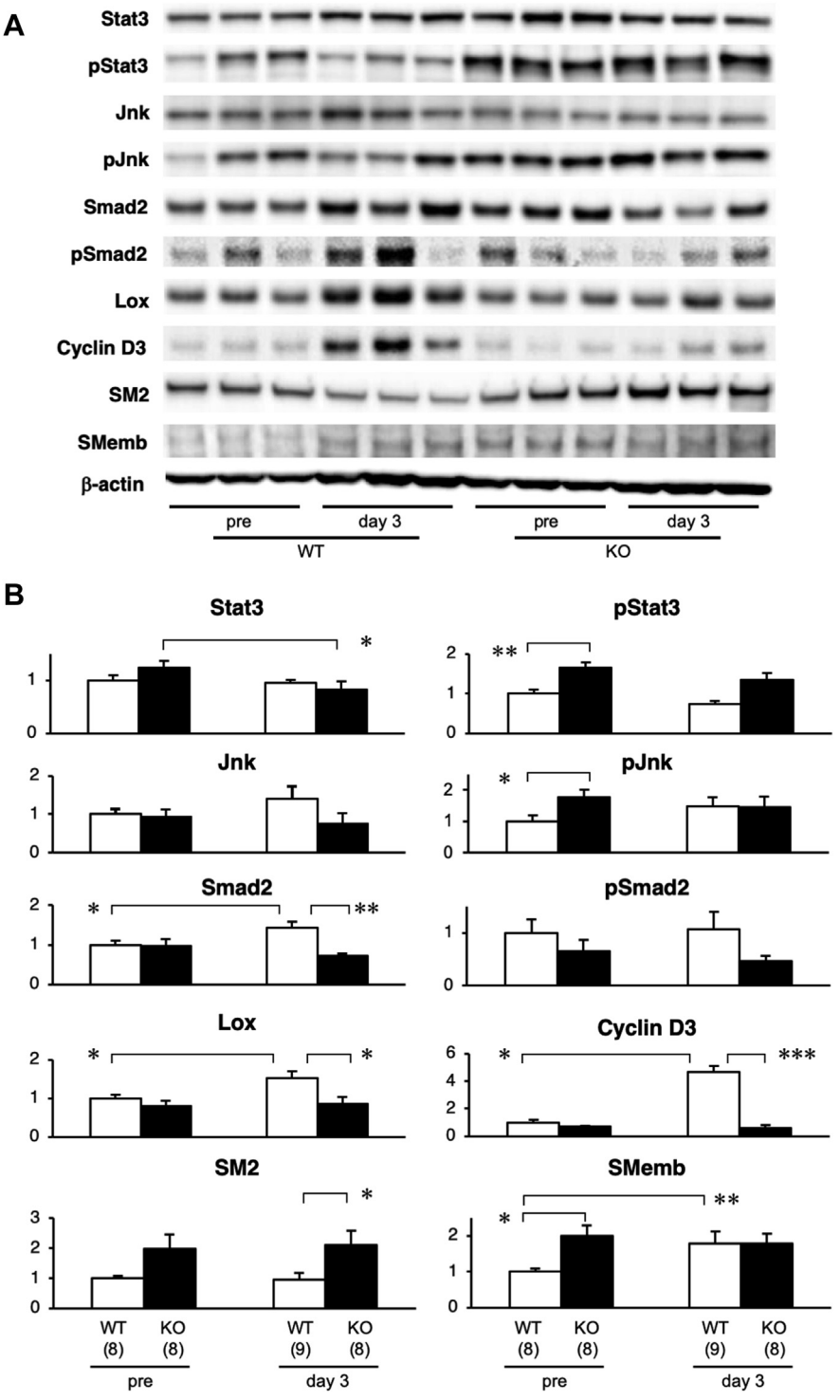


**(A)** Western blot shows expression levels of the indicated proteins in aortas from WT and KO mice, isolated before (pre) and 3 days after BAPN+AngII infusion. **(B)** Quantitative analyses of the relative expressions of aortic proteins, measured before and 3 days after BAPN+AngII infusion in aortic tissue from WT **(open columns)** and KO **(solid columns)** mice. All data are normalized to β-actin levels (internal loading control). The numbers of mice in each group are shown in parentheses. *$p < 0.05$; **$p < 0.01$; and ***$p < 0.001$. Jnk = c-Jun N-terminal kinases; Lox = lysyl oxidase; SM2 = smooth muscle myosin heavy chain; Smad2 = Mothers Against Decapentaplegic Homolog 2; SMemb = embryonic isoform of myosin heavy chain; other abbreviations as in Figures 1 and 2.

**FIGURE 6 Cell Proliferative Response in Aortic Tissue**

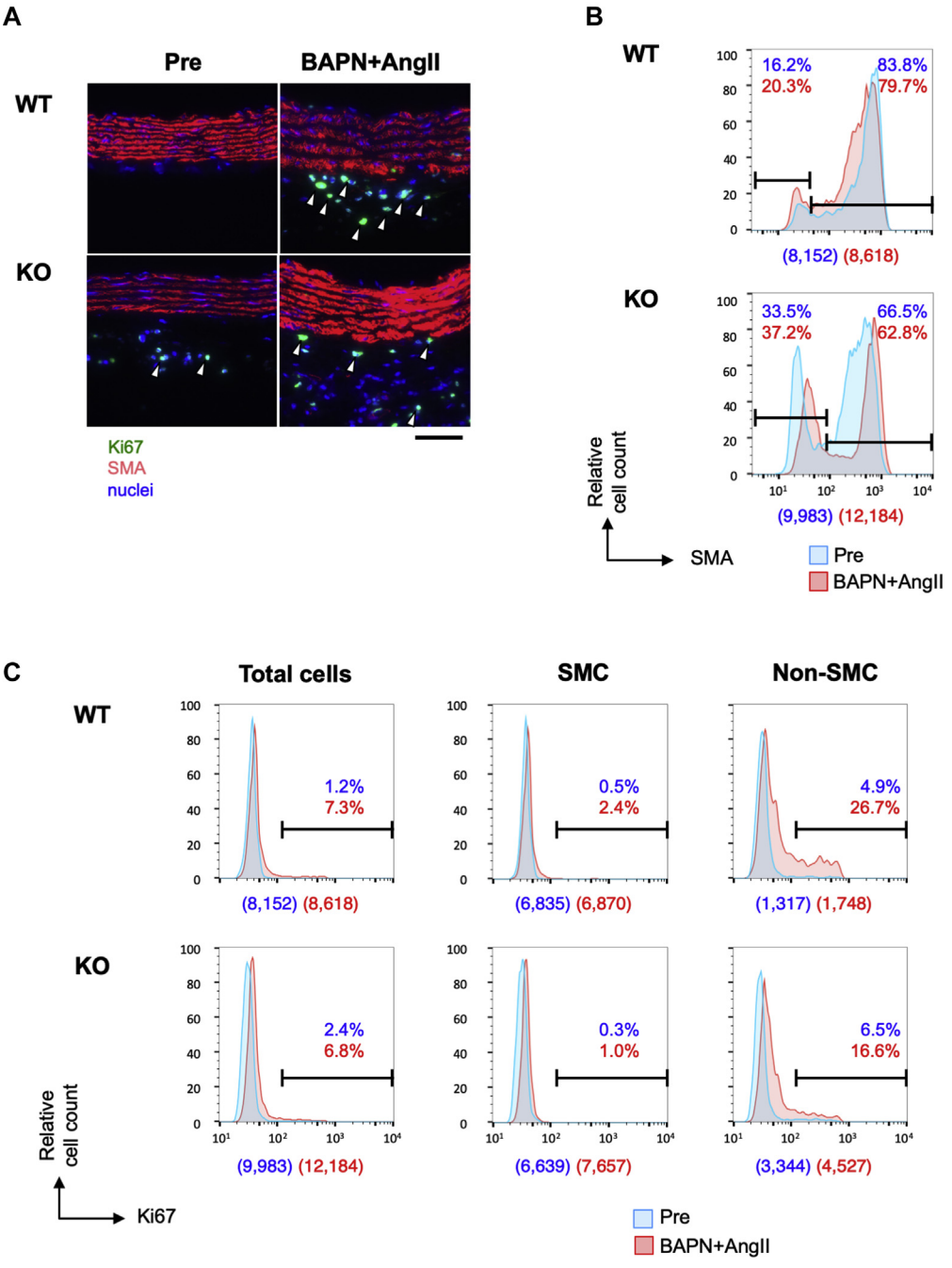


**(A)** Representative immunofluorescence-stained images show Ki67 **(green)** and SMA **(red)** expression, and nuclei (DAPI; **blue**) in aortic sections from **(upper)** WT or **(lower)** KO mice, before (Pre) and 3 days after BAPN+AngII infusion. **Arrowheads** indicate Ki67-positive nuclei. Bar = 50 μm. **(B)** Imaging cytometry results for SMA expression in aortic tissue from **(upper)** WT and **(lower)** KO mice, acquired before **(blue)** and 3 days after BAPN+AngII infusion **(red).** SMA-negative cells indicate non-SMC, and SMA-positive cells indicate SMC, as defined with arbitrarily delineated gates **(horizontal bars)** that remained constant for all samples. **(C)** Histograms show Ki67 detection in WT and KO aortas. SMC and non-SMC populations were defined with arbitrarily defined gates **(horizontal bars** in **B)** that remained constant for all samples. **Blue** and **red** proportion values indicate the proportions of cells within the gated sections among all analyzed cells in the Pre and BAPN+AngII samples, respectively. Numbers in parentheses below each histogram indicate the counted cell numbers without **(blue)** and with **(red)** BAPN+AngII. Abbreviations as in **Figures 1 and 2**.

deposition was more prominent in smSocs3-KO aortas than in WT aortas, both at baseline and after BAPN+AngII treatment. This fibrosis was particularly prominent in the adventitia adjacent to the media. We did not observe increases in perivascular fibrosis in coronary arteries of smSocs3-KO mice (Supplemental Figure S5), suggesting a differential effect of smooth muscle *Socs3* deletion on arterial collagen deposition within the vasculature. Overall, these findings indicated that *Socs3* deletion in SMC promoted adventitial fibrosis and increased fibroblasts in the aortic wall.

To measure the tensile strength of aortic walls before BAPN+AngII treatment, aortic rings were obtained from the distal aortic arches of WT and smSocs3-KO mice, and were stretched outwardly (Supplemental Figure S2). Simultaneous video and force recordings during this procedure revealed that the medial tensile strength did not significantly differ between WT and smSocs3-KO aortas (**Figure 7C**), whereas the tensile strength of the adventitia was higher in smSocs3-KO aortas than in WT aortas. These results suggested that the increases of fibroblasts and collagen deposition in the adventitia, caused by *Socs3* deletion in SMC, strengthened the adventitia of the aortic wall.

**INTERACTION BETWEEN SMC AND FIBROBLASTS.** To explore the potential mechanism underlying the interaction between smooth muscle Stat3 activation and fibroblast activation, we performed in vitro cell culture experiments using mouse aortic SMC and fibroblasts (**Figure 8**). We first obtained conditioned media by culturing SMC with or without stimulation by the Stat3 activator IL-6. Then we assessed the effects of treating fibroblast cultures with this conditioned media. We analyzed fibroblast proteins for tyrosine phosphorylation as a marker of growth response, and for pSmad2 as a marker of the fibrogenetic response. IL-6-stimulated SMC-conditioned media induced increases in tyrosine phosphorylation of multiple proteins in fibroblasts, and caused no significant changes in pSmad2. These results suggested that IL-6 caused SMC to secrete soluble factors that can induce growth response of fibroblasts.

## DISCUSSION

Our present results demonstrated that *Socs3* deletion in SMC resulted in Stat3 activation and changes in multiple molecular and cellular aortic phenotypes, which seemed to be related to each other. The mouse aortic transcriptome prior to BAPN+AngII challenge indicated that *Socs3* deletion in SMC was associated with activations of Stat3 and Jnk and increased inflammatory and defense responses. These baseline changes presumably reflected the presence of chronic inflammation in the aortic walls. Because chronic inflammation is associated with fibrosis (28), chronic Stat3 activation and the inflammatory response in smSocs3-KO aortas may explain the expansion of adventitial fibroblasts and deposition of collagen fibers observed in smSocs3-KO samples. Notably, the increase of fibroblasts was associated with the increased adventitial collagen deposition. The smSocs3-KO aortas also expressed elevated levels of SM2 (a marker of highly differentiated SMC) and SMemb (a marker of synthetic SMC and non-SMC). The elevated SMemb expression may have been due to the expansion of fibroblasts that expressed SMemb in the chronic inflammatory state (29), and the elevated SM2 expression may indicate maintained SMC differentiation in the smSocs3-KO aorta. Importantly, smooth muscle *Socs3* deletion provided the most evident protection against AD in the aortic arch, involvement of which is the major determinant of prognosis in human AD (30). Overall, our data indicated that *Socs3* deletion in SMC induced a chronic inflammatory response and adventitial fibrosis, resulting in reinforcement of tensile strength in the aortic adventitia at baseline.

In WT aortas, BAPN+AngII infusion for 3 days caused cell cycle activation, as demonstrated by increased Ki67-positive cells and cyclin D3 induction, without significant activation of the proinflammatory molecules Stat3 and Jnk. These findings were consistent with our previous report (18), showing that cell cycle activation preceded the inflammatory response in early stages of AD development. BAPN+AngII infusion also modulated the SMC phenotype in WT aorta, as demonstrated by SMA reduction and increased SMemb expression. In contrast, BAPN+AngII infusion did not alter cell cycle activation or modulate the SMC phenotype in smSocs3-KO aortas, suggesting that the reinforced adventitia protected SMC in smSocs3-KO aortas from the BAPN+AngII challenge. Human genetic studies have revealed that familial AD is caused by mutations in genes specifically expressed in differentiated SMC (19). Thus, maintenance of the differentiated SMC phenotype in smSocs3-KO mice may contribute to the protection from aortic dissection.

**FIGURE 7** **Collagen Deposition and Mechanical Properties of the Aortic Walls**

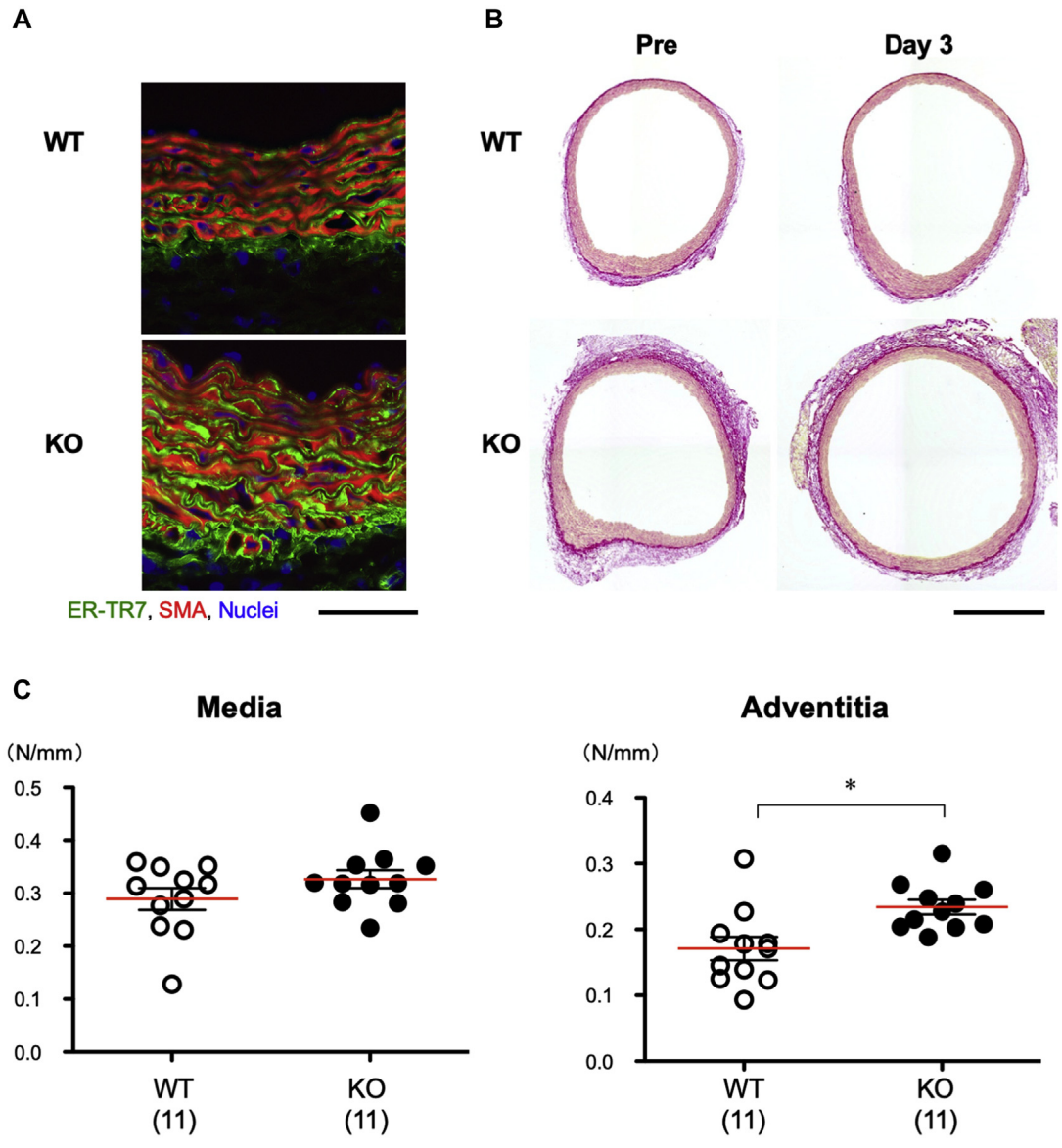


**(A)** Representative immunofluorescence-stained images show sections of aortas from WT and KO mice. Aortas were isolated before BAPN+AngII treatment. ER-TR7 is a fibroblast marker **(green)** and SMA **(red)** is specific for SMC. Bar = 50 μm. **(B)** Representative images show picrosirius red staining of collagen fibers in WT and KO aortic rings, before (Pre) and 3 days after BAPN+AngII treatment. Bar = 0.5 mm. **(C)** Maximal tensile forces (N/mm width of aortic ring) in the medial and adventitial layers of aortic rings isolated from WT **(open circles)** and KO **(solid circles)** mice, before BAPN+AngII treatment. The numbers of mice in each group are shown in parentheses. **Red bars** indicate mean values. *$p < 0.05$. Abbreviations as in **Figures 1 and 2**.

Our current findings seemed to suggest that the Socs3-regulated response in SMC (possibly a Stat3-dependent process) might be regarded as a mechanism that protects aortic tissues against insults that can cause AD. We previously reported that stress-induced expression of tenascin C was another mechanism that reinforced aortic tissues and prevented AD development (12). Notably, tenascin C is a known target of Stat3 (31), which promotes collagen deposition in various tissues (32). Another report shows that high levels of serum tenascin C are associated with aortic tissue stabilization in chronic AD

**FIGURE 8** SMC-Fibroblast Interaction

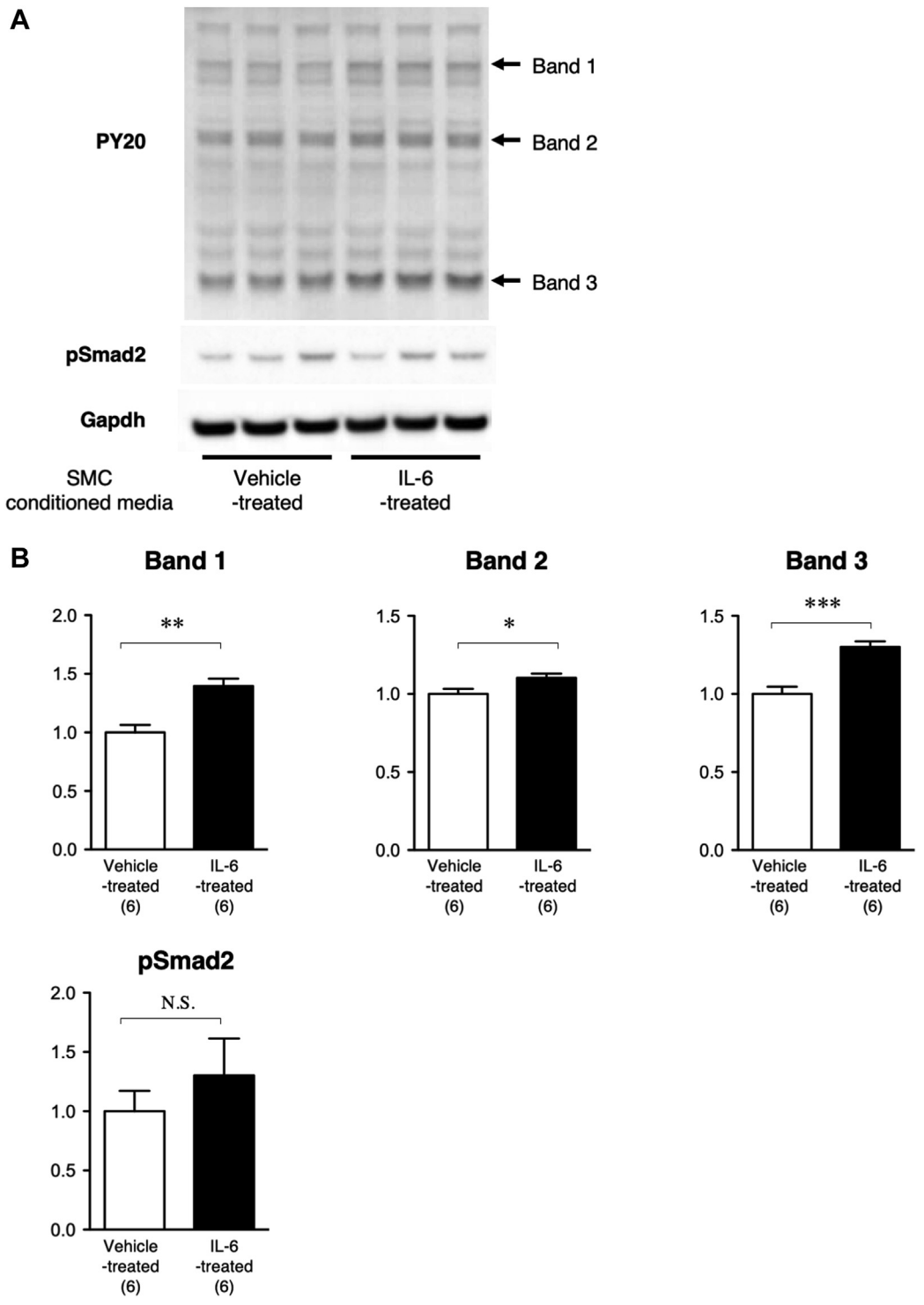


**(A)** Representative immunoblot images are shown for phosphotyrosine (PY20), phospho-Smad2 (pSmad2), and glyceraldehyde 3-phosphate dehydrogenase (Gapdh; internal control). **(B)** Quantitative analysis is shown for bands 1 to 3 (as indicated by **arrows** in PY20 immunoblot) and for pSmad2. The data were normalized against the Gapdh signal and expressed as relative to the value of the vehicle-treated group. *$p < 0.05$; **$p < 0.01$; and ***$p < 0.001$. IL-6 = interleukin-6. Abbreviations as in Figures 2, 4, and 5.

(33). Moreover, Stat3 activation is reportedly involved in fibrosis in renal (34), atrial (35), and pulmonary tissues (36). Overall, these findings suggest that Stat3 might play an important role in fibrosis, which is in accordance with our present findings that a *Socs3* deletion in SMC was associated with increased fibrous collagen deposition in the aortic adventitia. Consistently, compared with WT aortas, smSocs3-KO aortas showed higher expression of the markers of M2 macrophages that play an important role in tissue repair and fibrosis (37). The aorta must endure high mechanical stress due to blood pressure and pulsatile flow; thus, a mechanism for maintaining the physical strength of aortic walls is critical. Our present results suggested that Stat3 may be an important component in the mechanism for maintaining aortic wall integrity.

In contrast to our present finding that Stat3 activation in SMC was protective against AD development, previous studies report that IL-6 (a well-established ligand for Stat3 activation) promotes AD by amplifying inflammation (4,6,7) and a Stat3 inhibitor suppresses AngII-induced AD development in mice (38). These prior findings suggest that Stat3 activation can promote AD development. Consistent with those reports, we recently observed that macrophage-specific *Socs3* deletion promotes AD development (18) due to the Stat3-dependent differentiation of macrophages toward proinflammatory and destructive M1 phenotypes (39). On the other hand, Stat3-activating ligands, including IL-6, play important roles in tissue repair (28). For example, IL-6 (40) and Stat3 (41) are essential in skin wound healing, where they promote keratinocyte proliferation and growth, and Stat3 activation promotes cell proliferation and inhibits apoptosis of SMC (42). Intriguingly, diabetes mellitus, a known negative risk factor for thoracic AD (43), is reportedly associated with Jak/Stat pathway activation in the thoracic aorta (44). Overall, the current findings, together with our previous report (18), suggest that Socs3 function in AD pathogenesis varies among different cell types. Socs3 in SMC prevented both chronic inflammation and aortic tissue reinforcement, whereas Socs3 in macrophages prevents tissue destruction and AD development. Whether these cell-type-specific functions of Socs3 are beneficial or detrimental to tissue integrity depends on the disease context.

**STUDY LIMITATIONS.** Our study demonstrated that smSocs3-KO aorta showed fibroblast activation, collagen fiber deposition and reinforced tensile strength of aortic adventitia, as well as ameliorated AD phenotype. Although these are likely to make a sequential event, this interpretation awaits formal proof in the context of AD. Likewise, the molecular mechanism of medial SMC-mediated regulation of adventitial fibroblast activation remains to be elucidated. The reinforcement of adventitia may not be the only mechanism for AD amelioration in smSocs3-KO mice. Indeed, the gene expression analysis of immune cell markers suggested the altered immunological response in smSocs3-KO aorta, which is likely to contribute to the observed AD phenotype. These unsolved questions need to be addressed in future studies.

## CONCLUSIONS

The current understanding of the molecular pathogenesis of AD is that tissue destruction is driven by inflammatory response, possibly through the secretion of tissue-degrading proteases by infiltrating cells (4,5,7,38). The direct clinical implication of this understanding is that inflammatory response inhibition may be a therapeutic strategy for AD. However, our present findings indicated that *Socs3* deletion in SMC protected the aorta against AD, even though it caused activation of a low-grade inflammatory response (e.g., IL-6 expression and Stat3 activation) in the aortic walls. This low-grade inflammatory response in SMC seems to be a built-in protective mechanism in the aorta, suggesting that inflammatory response inhibition might not only suppress the tissue destruction but also hinder the tissue-protective mechanism. An ideal therapeutic strategy would allow inhibition of the tissue-destructive response, while enhancing the tissue-protective response. Further investigations are required to elucidate the tissue-destructive and -protective mechanisms and how these mechanisms are coordinated in AD pathogenesis.

**ACKNOWLEDGMENTS** The authors would like to thank Ms. Kiyohiro, Ms. Nishigata, Ms. Nakao, Ms. Shiramizu, Ms. Nakayama, and Dr. Yamamoto for technical assistance.

**ADDRESS FOR CORRESPONDENCE:** Dr. Hiroki Aoki, Cardiovascular Research Institute, Kurume University, 67 Asahimachi, Kurume, Fukuoka 830-0011, Japan. E-mail: haoki@med.kurume-u.ac.jp.

## PERSPECTIVES

**COMPETENCY IN MEDICAL KNOWLEDGE:** AD is a major cause of acute aortic syndrome that occurs without preceding signs or symptoms and often leads to sudden death due to the aortic wall destruction. It has been proposed that inflammation plays a central role in AD by destructing ECM. However, inflammation is a complex process that involves various cell types that communicate with each other through cytokines and cellular signaling pathways. We showed that SMC-specific enhancement of Stat3 signaling, a major pathway for proinflammatory cytokines, by genetic deletion of Socs3, a negative regulator of Stat3 signaling, protected the aorta from AD. Stat3 activation in SMC resulted in secretion of humoral factor(s) that activated fibroblasts. This process contributed to the accumulation of adventitial collagen fibers and reinforcement of the tensile strength to protect aorta from AD. These findings suggest that inflammatory response involves not only ECM destruction but also ECM biosynthesis that is regulated by Stat3 signaling in SMC, and AD is a consequence of the imbalance of ECM metabolism.

**TRANSLATIONAL OUTLOOK:** Our findings suggest that inflammatory response involves not only ECM destruction but also ECM biosynthesis, and AD is a consequence of the imbalance of ECM metabolism. For the clinical translation, how these finding can be applied to the time course of human AD needs to be addressed. AD is characterized by the sudden aortic wall destruction with high mortality in the acute phase. However, even those who survived the acute phase suffer from aortic complications including aneurysmal expansion of the aorta and malperfusion of distal organs due to the progressive aortic wall destruction. The regulatory mechanisms for the balance of ECM destruction and biosynthesis need to be clarified in the context of the AD time course. Such a knowledge will help to develop the strategies to monitor the balance of ECM metabolism, prevent the excessive ECM destruction, and promote the desirable ECM biosynthesis at the appropriate time points in the time course of AD.

## REFERENCES

**1.** Erbel R, Aboyans V, Boileau C, et al. 2014 ESC Guidelines on the diagnosis and treatment of aortic diseases. Eur Heart J 2014;35:2873–926.

**2.** Evangelista A, Isselbacher EM, Bossone E, et al., for the IRAD Investigators. Insights from the International Registry of Acute Aortic Dissection: a 20-year experience of collaborative clinical research. Circulation 2018;137:1846–60.

**3.** Tsai TT, Evangelista A, Nienaber CA, et al. Long-term survival in patients presenting with type A acute aortic dissection: insights from the International Registry of Acute Aortic Dissection (IRAD). Circulation 2006;114:I350–6.

**4.** Tieu BC, Lee C, Sun H, et al. An adventitial IL-6/MCP1 amplification loop accelerates macrophage-mediated vascular inflammation leading to aortic dissection in mice. J Clin Invest 2009;119:3637–51.

**5.** Kurihara T, Shimizu-Hirota R, Shimoda M, et al. Neutrophil-derived matrix metalloproteinase 9 triggers acute aortic dissection. Circulation 2012;126:3070–80.

**6.** Son BK, Sawaki D, Tomida S, et al. Granulocyte macrophage colony-stimulating factor is required for aortic dissection/intramural haematoma. Nat Commun 2015;6:6994.

**7.** Anzai A, Shimoda M, Endo J, et al. Adventitial CXCL1/G-CSF expression in response to acute aortic dissection triggers local neutrophil recruitment and activation leading to aortic rupture. Circ Res 2015;116:612–23.

**8.** Fan LM, Douglas G, Bendall JK, et al. Endothelial cell-specific reactive oxygen species production increases susceptibility to aortic dissection. Circulation 2014;129:2661–72.

**9.** Gavazzi G, Deffert C, Trocme C, Schappi M, Herrmann FR, Krause KH. NOX1 deficiency protects from aortic dissection in response to angiotensin II. Hypertension 2007;50:189–96.

**10.** Rahkonen O, Su M, Hakovirta H, et al. Mice with a deletion in the first intron of the Col1a1 gene develop age-dependent aortic dissection and rupture. Circ Res 2004;94:83–90.

**11.** Smith LB, Hadoke PW, Dyer E, et al. Haploinsufficiency of the murine Col3a1 locus causes aortic dissection: a novel model of the vascular type of Ehlers-Danlos syndrome. Cardiovasc Res 2011;90:182–90.

**12.** Kimura T, Shiraishi K, Furusho A, et al. Tenascin C protects aorta from acute dissection in mice. Sci Rep 2014;4:4051.

**13.** Maki J, Rasanen J, Tikkanen H, et al. Inactivation of the lysyl oxidase gene Lox leads to aortic aneurysms, cardiovascular dysfunction, and perinatal death in mice. Circulation 2002;106:2503–9.

**14.** Lee VS, Halabi CM, Hoffman EP, et al. Loss of function mutation in LOX causes thoracic aortic aneurysm and dissection in humans. Proc Natl Acad Sci U S A 2016;113:8759–64.

**15.** de Figueiredo Borges L, Jaldin RG, Dias RR, Stolf NA, Michel JB, Gutierrez PS. Collagen is reduced and disrupted in human aneurysms and dissections of ascending aorta. Hum Pathol 2008;39:437–43.

**16.** Wang X, LeMaire SA, Chen L, et al. Decreased expression of fibulin-5 correlates with reduced elastin in thoracic aortic dissection. Surgery 2005;138:352–9.

**17.** Xu J, Shi GP. Vascular wall extracellular matrix proteins and vascular diseases. Biochim Biophys Acta 2014;1842:2106–19.

**18.** Ohno-Urabe S, Aoki H, Nishihara M, et al. Role of macrophage Socs3 in the pathogenesis of aortic dissection. J Am Heart Assoc 2018;7:e007389.

**19.** Brownstein AJ, Ziganshin BA, Kuivaniemi H, Body SC, Bale AE, Elefteriades JA. Genes associated with thoracic aortic aneurysm and dissection: an update and clinical implications. Aorta (Stamford) 2017;5:11–20.

**20.** Nienaber CA, Fattori R, Mehta RH, et al., for the International Registry of Acute Aortic Dissection. Gender-related differences in acute aortic dissection. Circulation 2004;109:3014–21.

**21.** Yasukawa H, Ohishi M, Mori H, et al. IL-6 induces an anti-inflammatory response in the absence of SOCS3 in macrophages. Nat Immunol 2003;4:551–6.

**22.** Logghe G, Trachet B, Aslanidou L, et al. Propagation-based phase-contrast synchrotron imaging of aortic dissection in mice: from individual elastic lamella to 3D analysis. Sci Rep 2018;8:2223.

**23.** DAVID Bioinformatics Database. DAVID Bioinformatics Resource 6.8. Laboratory of Human Retrovirology and Immunoinformatics (LHRI). Available at: https://david.ncifcrf.gov/. Accessed December 18, 2016.

**24.** Huang da W, Sherman BT, Lempicki RA. Systematic and integrative analysis of large gene lists using DAVID bioinformatics resources. Nat Protoc 2009;4:44–57.

**25.** Waurick R, Knapp J, Van Aken H, Boknik P, Neumann J, Schmitz W. Effect of 2,3-butanedione monoxime on force of contraction and protein phosphorylation in bovine smooth muscle. Naunyn Schmiedebergs Arch Pharmacol 1999;359:484–92.

**26.** DiRocco DP, Kobayashi A, Taketo MM, McMahon AP, Humphreys BD. Wnt4/beta-catenin signaling in medullary kidney myofibroblasts. J Am Soc Nephrol 2013;24:1399–412.

**27.** Pan S, Wu D, Teschendorff AE, et al. JAK2-centered interactome hotspot identified by an integrative network algorithm in acute Stanford type A aortic dissection. PLoS One 2014;9:e89406.

**28.** O'Reilly S, Ciechomska M, Cant R, Hugle T, van Laar JM. Interleukin-6, its role in fibrosing conditions. Cytokine Growth Factor Rev 2012;23:99–107.

**29.** Santiago JJ, Dangerfield AL, Rattan SG, et al. Cardiac fibroblast to myofibroblast differentiation in vivo and in vitro: expression of focal adhesion components in neonatal and adult rat ventricular myofibroblasts. Dev Dyn 2010;239:1573–84.

**30.** Crawford ES. The diagnosis and management of aortic dissection. JAMA 1990;264:2537–41.

**31.** Azare J, Leslie K, Al-Ahmadie H, et al. Constitutively activated Stat3 induces tumorigenesis and enhances cell motility of prostate epithelial cells through integrin beta 6. Mol Cell Biol 2007;27:4444–53.

**32.** Imanaka-Yoshida K. Tenascin-C in cardiovascular tissue remodeling: from development to inflammation and repair. Circ J 2012;76:2513–20.

**33.** Nozato T, Sato A, Hikita H, et al. Impact of serum tenascin-C on the aortic healing process during the chronic stage of type B acute aortic dissection. Int J Cardiol 2015;191:97–9.

**34.** Choi HI, Ma SK, Bae EH, Lee J, Kim SW. Peroxiredoxin 5 protects TGF-beta induced fibrosis by inhibiting Stat3 activation in rat kidney interstitial fibroblast cells. PLoS One 2016;11:e0149266.

**35.** Huang Z, Chen XJ, Qian C, et al. Signal transducer and activator of transcription 3/microRNA-21 feedback loop contributes to atrial fibrillation by promoting atrial fibrosis in a rat sterile pericarditis model. Circ Arrhythm Electrophysiol 2016;9:e003396.

**36.** Pedroza M, Le TT, Lewis K, et al. STAT-3 contributes to pulmonary fibrosis through epithelial injury and fibroblast-myofibroblast differentiation. FASEB J 2016;30:129–40.

**37.** Das A, Sinha M, Datta S, et al. Monocyte and macrophage plasticity in tissue repair and regeneration. Am J Pathol 2015;185:2596–606.

**38.** Ju X, Ijaz T, Sun H, et al. Interleukin-6-signal transducer and activator of transcription-3 signaling mediates aortic dissections induced by angiotensin II via the T-helper lymphocyte 17-interleukin 17 axis in C57BL/6 mice. Arterioscler Thromb Vasc Biol 2013;33:1612–21.

**39.** Qin H, Holdbrooks AT, Liu Y, Reynolds SL, Yanagisawa LL, Benveniste EN. SOCS3 deficiency promotes M1 macrophage polarization and inflammation. J Immunol 2012;189:3439–48.

**40.** Gallucci RM, Simeonova PP, Matheson JM, et al. Impaired cutaneous wound healing in interleukin-6-deficient and immunosuppressed mice. FASEB J 2000;14:2525–31.

**41.** Li D, Wang A, Liu X, et al. MicroRNA-132 enhances transition from inflammation to proliferation during wound healing. J Clin Invest 2015;125:3008–26.

**42.** Shibata R, Kai H, Seki Y, et al. Inhibition of STAT3 prevents neointima formation by inhibiting proliferation and promoting apoptosis of neointimal smooth muscle cells. Hum Gene Ther 2003;14:601–10.

**43.** LeMaire SA, Russell L. Epidemiology of thoracic aortic dissection. Nat Rev Cardiol 2011;8:103–13.

**44.** Banes-Berceli AK, Ketsawatsomkron P, Ogbi S, Patel B, Pollock DM, Marrero MB. Angiotensin II and endothelin-1 augment the vascular complications of diabetes via JAK2 activation. Am J Physiol Heart Circ Physiol 2007;293:H1291–9.

**KEY WORDS** aortic dissection, inflammation, Jak/Stat, smooth muscle cells

**APPENDIX** For supplemental figures and tables, please see the online version of this paper.